

University of Windsor

Scholarship at UWindor

Electronic Theses and Dissertations

Theses, Dissertations, and Major Papers

1-1-1967

M(J) mixing in oriented $4(2)P(1/2)$ potassium atoms, induced by collisions with inert gases.

John D. Guiry
University of Windsor

Follow this and additional works at: <https://scholar.uwindsor.ca/etd>

Recommended Citation

Guiry, John D., "M(J) mixing in oriented $4(2)P(1/2)$ potassium atoms, induced by collisions with inert gases." (1967). *Electronic Theses and Dissertations*. 6481.
<https://scholar.uwindsor.ca/etd/6481>

This online database contains the full-text of PhD dissertations and Masters' theses of University of Windsor students from 1954 forward. These documents are made available for personal study and research purposes only, in accordance with the Canadian Copyright Act and the Creative Commons license—CC BY-NC-ND (Attribution, Non-Commercial, No Derivative Works). Under this license, works must always be attributed to the copyright holder (original author), cannot be used for any commercial purposes, and may not be altered. Any other use would require the permission of the copyright holder. Students may inquire about withdrawing their dissertation and/or thesis from this database. For additional inquiries, please contact the repository administrator via email (scholarship@uwindsor.ca) or by telephone at 519-253-3000ext. 3208.

M_J MIXING IN ORIENTED $4^2P_{1/2}$ POTASSIUM ATOMS,
INDUCED BY COLLISIONS WITH INERT GASES

by

John D. Guiry

A Thesis

Submitted to the Faculty of Graduate Studies through the Department
of Physics in Partial Fulfillment of the Requirements for
the Degree of Master of Science at the
University of Windsor

Windsor, Ontario

1967

UMI Number: EC52662

INFORMATION TO USERS

The quality of this reproduction is dependent upon the quality of the copy submitted. Broken or indistinct print, colored or poor quality illustrations and photographs, print bleed-through, substandard margins, and improper alignment can adversely affect reproduction.

In the unlikely event that the author did not send a complete manuscript and there are missing pages, these will be noted. Also, if unauthorized copyright material had to be removed, a note will indicate the deletion.

UMI[®]

UMI Microform EC52662

Copyright 2008 by ProQuest LLC.

All rights reserved. This microform edition is protected against unauthorized copying under Title 17, United States Code.

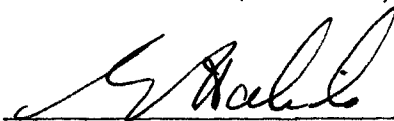
ProQuest LLC
789 E. Eisenhower Parkway
PO Box 1346
Ann Arbor, MI 48106-1346

ABB4541

APPROVED BY:



Dr. L. Krause (Chairman)



Dr. E. E. Habib

177175



Dr. R. J. Thibert

ABSTRACT

A modified Zeeman scanning method was used to excite selectively the magnetic sublevels of the $4^2P_{1/2}$ resonance states in potassium atoms mixed with inert gases and placed in a strong magnetic field. The resulting potassium-inert gas atomic collisions induced m_J mixing in potassium, which manifested itself by the depolarization of the potassium resonance fluorescence. The polarization measurements yielded the following disorientation cross sections: K - He: 46 \AA^2 ; K - Ne: 39 \AA^2 ; K - Ar: 52 \AA^2 ; K - Kr: 79 \AA^2 ; K - Xe: 108 \AA^2 .

ACKNOWLEDGEMENTS

I would like to thank Dr. L. Krause for his guidance during the past year and for the time spent in correction of the original manuscript. I should also like to express my gratitude to Dr. W. Berdowski for his invaluable guidance and advice and to Mr. T. Shiner for his assistance.

The success of the experimental work owes much to Mr. D. Cox, who maintained the electronic equipment; to Master Glassblower W. Eberhart, who manufactured the fluorescence cell, and to Mr. W. Grewe who constructed the photomultiplier cryostat and other pieces of equipment.

TABLE OF CONTENTS

	Page
ABSTRACT	iii
ACKNOWLEDGEMENTS	iv
LIST OF TABLES	vi
LIST OF FIGURES	vii
I. INTRODUCTION	1
II. THE PRINCIPLE OF ZEEMAN SCANNING	3
III. THE RATE PROCESSES GOVERNING COLLISIONAL DISALIGNMENT OF MAGNETICALLY ORIENTED POTASSIUM ATOMS	7
IV. THE DESCRIPTION OF THE APPARATUS	12
(i) The Spectral Lamp	12
(ii) The Electromagnets	14
(iii) The Fluorescence Cell	17
(iv) The Optical System	19
(v) The Vacuum and Gas-Filling System	22
V. EXPERIMENTAL PROCEDURE	25
VI. RESULTS AND DISCUSSION	31
BIBLIOGRAPHY	39
VITA AUCTORIS	40

LIST OF TABLES

	Page
1. Collision Cross Section for $m_J = -1/2 \longrightarrow m_J = +1/2$ Mixing in the $4^2P_{1/2}$ State of Potassium	32

LIST OF FIGURES

	Page
1. The Selective Excitation of Resonance Fluorescence in the Zeeman Components of the $4^2P_{1/2}$ Level in Potassium	4
2. Fluorescence from the $4^2P_{1/2}$ Level in Pure Potassium Vapour Excited with σ^- Light	6
3. Transitions Between the Zeeman Levels of the Ground and Resonance States	8
4. Arrangement of the Apparatus	13
5. Arrangement of the Electromagnets	15
6. The Fluorescence Cell	18
7. Cell in Main Oven	20
8. The Vacuum and Gas-Filling System	23
9. Fluorescence from the $4^2P_{1/2}$ Level in Potassium Vapour Mixed with Argon, Excited with σ^- Light	30
10. The Degrees of Polarization of the 7699 Å Resonance Fluorescence, Plotted as Functions of Inert Gas Pressures	34
11. Plots of Collision Numbers Against the Pressures of Inert Gases	36
12. A Comparison of Disorientation Cross Sections Q for Potassium-Inert Gas Collisions with the Elastic Electron Scattering Cross Sections	38

I. INTRODUCTION

When a mixture of potassium vapour and an inert gas is irradiated with one component of the potassium resonance doublet, the fluorescent light will consist of the component present in the incident light (resonance fluorescence) as well as those components which arise as a result of collisional excitation energy transfer (sensitized fluorescence). Such studies of inelastic atomic collisions provide information regarding the nature of inter-atomic forces. Experiments of this type, conducted at very low alkali vapour pressure to minimize the possibility of multiple absorption and re-emission of resonance radiation (radiation trapping), have been performed using vapours of potassium¹, rubidium² and cesium³ and their mixtures with inert gases^{1,4,5}. Investigations of collisional excitation transfer between the $^2P_{1/2}$ and $^2P_{3/2}$ resonance states in alkali atoms⁶ have led to speculation about the possible existence of selection rules governing collisional transitions between the Zeeman sublevels within a fine structure state and also between the Zeeman sublevels of two fine structure states^{7,8}.

To consider this matter in more detail, a series of experiments was proposed in which, by exciting selected Zeeman levels of either the $^2P_{1/2}$ or $^2P_{3/2}$ resonance state in alkali atoms mixed with an inert gas and placed in a strong magnetic field (sufficient to produce complete Paschen-Back Effect of the hfs), and

monitoring fluorescence arising from both optically and collisionally populated Zeeman sublevels, it should be possible to determine the cross sections for transitions between m_J states (disorientation cross sections) and to reach conclusions about the possible existence of selection rules.

The present investigation used a modified Zeeman scanning method⁹ in which, for the first time¹⁰, both the light source and fluorescence cell were placed in magnetic fields. The σ^- components of the 7699 Å potassium resonance line were used to excite the fluorescence which consisted not only of the expected σ^- resonance component but also contained a σ^+ component arising from collision-induced mixing. By monitoring the change in the degree of polarization with inert gas pressure, it was possible to determine the collision cross section $Q_{-\frac{1}{2},\frac{1}{2}}$ or $Q_{\frac{1}{2},-\frac{1}{2}}$ induced by inert gas collisions. While such cross sections do not directly yield information concerning the existence of selection rules, further experiments dealing with m_J mixing in the $^2P_{3/2}$ level are expected to provide more direct information on this matter¹¹.

II. THE PRINCIPLE OF ZEEMAN SCANNING

The optical excitation of m_J sublevels proceeds as follows. Light emitted from a potassium spectral lamp located in a constant magnetic field, M_1 , of 5 kG is made incident on potassium vapour at low pressure, contained in the fluorescence cell placed in a parallel magnetic field, M_2 , variable from 0 to 10 kG. Interference filters in the exciting beam transmit only the 7699 Å resonance component. Light emitted by the lamp in a direction parallel to the magnetic field M_1 is selected according to σ^- or σ^+ polarization by a circular polarizer which also changes the polarization of the linearly polarized σ and π components emitted perpendicularly to the field from linear to circular. In this way, there are two possible excitation methods: excitation by pure σ^+ or σ^- components corresponding to $\Delta m_J = +1$ or -1 selection rules, respectively, or by a circularly polarized $\pi - \sigma$ mixture corresponding to $\Delta m_J = 0, \pm 1$. In all cases, the exciting beam is perpendicular to the magnetic field M_2 . As the magnetic field M_2 is increased, with the exciting light emitted perpendicularly to the field M_1 , three coincidences, shown in Fig. 1, arise between the Zeeman sublevels in emission and in absorption. The central peak is due to resonances between corresponding σ and π components in emission and absorption while the other peaks arise from excitation by σ and π components of π and σ fluorescence, respectively.

For exciting light emitted parallel to M_1 , the corresponding

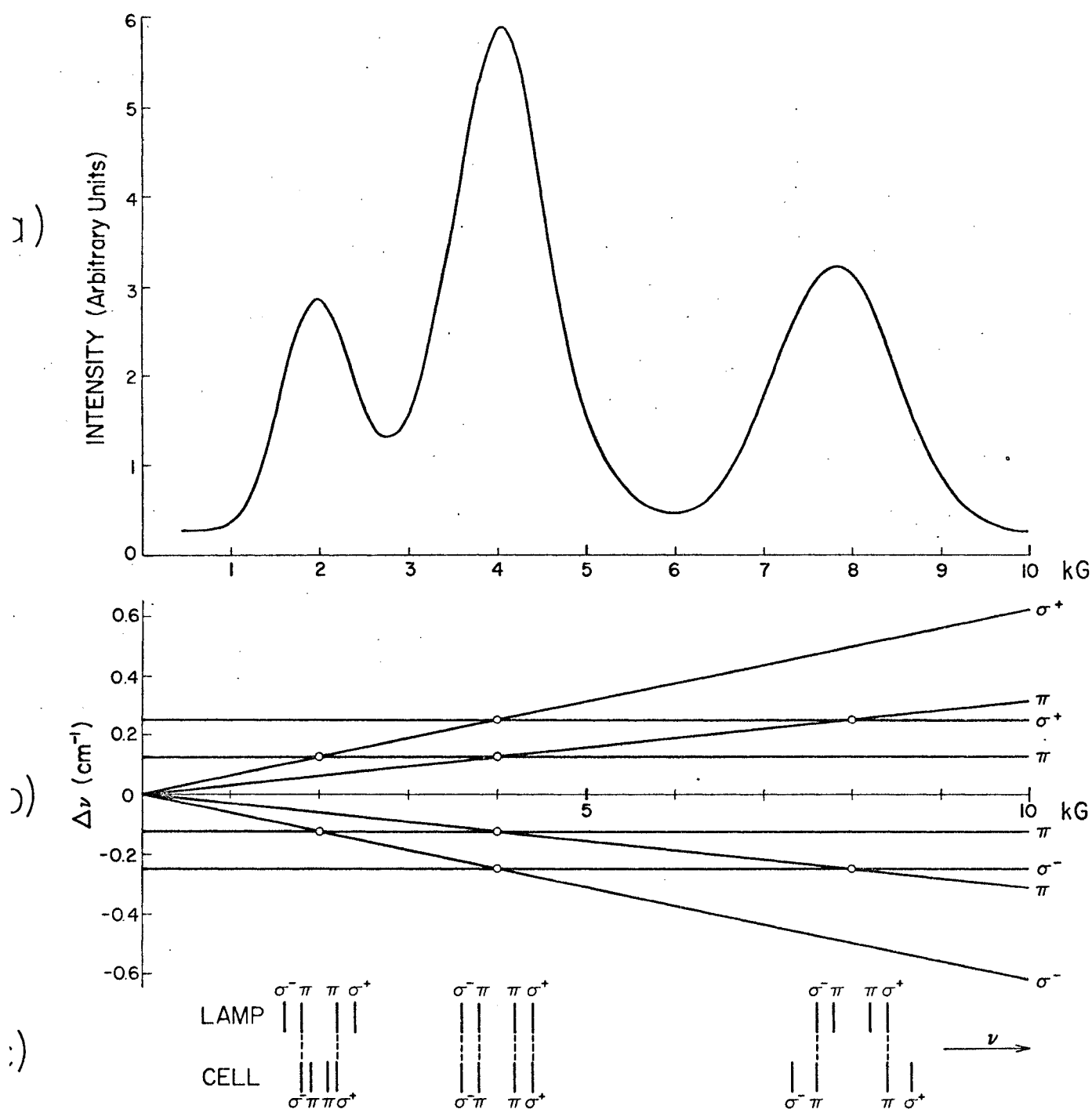


Fig. 1. The selective excitation of resonance fluorescence in the Zeeman components of the $4^2P_{1/2}$ level in potassium. (a) The experimental intensity profile of the σ component (the π component appears identical). (b) The Zeeman splitting of the 7699 Å line in the lamp (constant at 4 kG) and in the cell (variable). (c) Resonances between Zeeman components in the lamp and fluorescence cell.

fluorescent intensity profiles are shown in Fig. 2. Using σ^- excitation and observing the σ^- fluorescent component, the expected central peak is observed along with a smaller peak at 2.5 kG which is due principally to π impurity in the exciting beam. The weak σ^+ component present in the fluorescence is due to some σ^+ impurity in the exciting light and to imperfections in the circular analyzer located in the fluorescent beam.

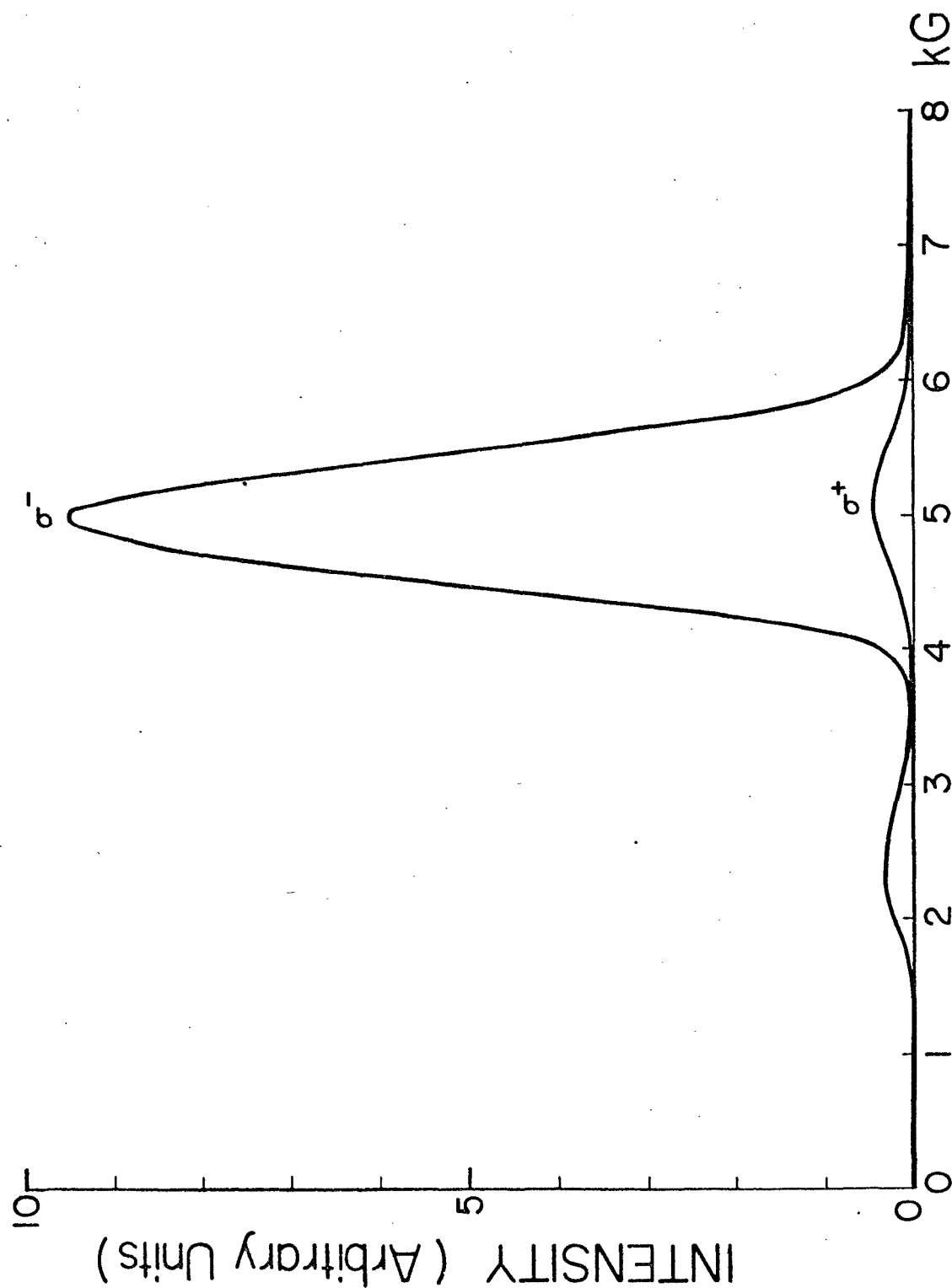


Fig. 2. Fluorescence from the $4^2P_{1/2}$ level in pure K vapor excited with σ^- light. The peak at 2.5 kG and the σ^+ component arise from a π impurity in the exciting radiation. 6

III. THE RATE PROCESSES GOVERNING COLLISIONAL DISORIENTATION OF MAGNETICALLY ORIENTED POTASSIUM ATOMS

Collisions between the excited potassium atoms in their Zeeman substates and inert gas atoms, cause mixing of the various sublevels according to the following equation:

$$(1) \quad K(4^2P_{\frac{1}{2}, -\frac{1}{2}}) + X(^1S_0) + \Delta E \rightleftharpoons K(4^2P_{\frac{1}{2}, \frac{1}{2}}) + X(^1S_0),$$

where $K(4^2P_{\frac{1}{2}, -\frac{1}{2}})$ refers to a potassium atom in its $4^2P_{1/2}$ resonance state and $m_J = -1/2$ Zeeman substate, $X(^1S_0)$ is an inert gas atom in its ground state, ΔE is the energy defect between the two substates $m_J = 1/2$, $m_J = -1/2$, the magnitude of which is dependent on the magnetic field strength. These collisions result in the depolarization of the resonance fluorescence, which is further increased by collisional transitions from the sublevels of the $^2P_{1/2}$ state to those of the $^2P_{3/2}$ state as indicated in Fig. 3. A study of such depolarization should yield values for m_J mixing cross sections.

The vapour-gas mixture is considered to exist in a state of dynamic equilibrium which can be represented by the following equations:

$$(2) \quad \frac{dn_{-\frac{1}{2}}}{dt} = -\frac{1}{\tau} n_{-\frac{1}{2}} - Z_{-\frac{1}{2}, \frac{1}{2}} n_{-\frac{1}{2}} + Z_{\frac{1}{2}, -\frac{1}{2}} n_{\frac{1}{2}} - Z_{12} n_{-\frac{1}{2}} + \frac{1}{2} Z_{21} N_2 + S_{-\frac{1}{2}} = 0,$$

$$(3) \quad \frac{dn_{\frac{1}{2}}}{dt} = -\frac{1}{\tau} n_{\frac{1}{2}} - Z_{\frac{1}{2}, -\frac{1}{2}} n_{\frac{1}{2}} + Z_{-\frac{1}{2}, \frac{1}{2}} n_{-\frac{1}{2}} - Z_{12} n_{\frac{1}{2}} + \frac{1}{2} Z_{21} N_2 + S_{\frac{1}{2}} = 0,$$

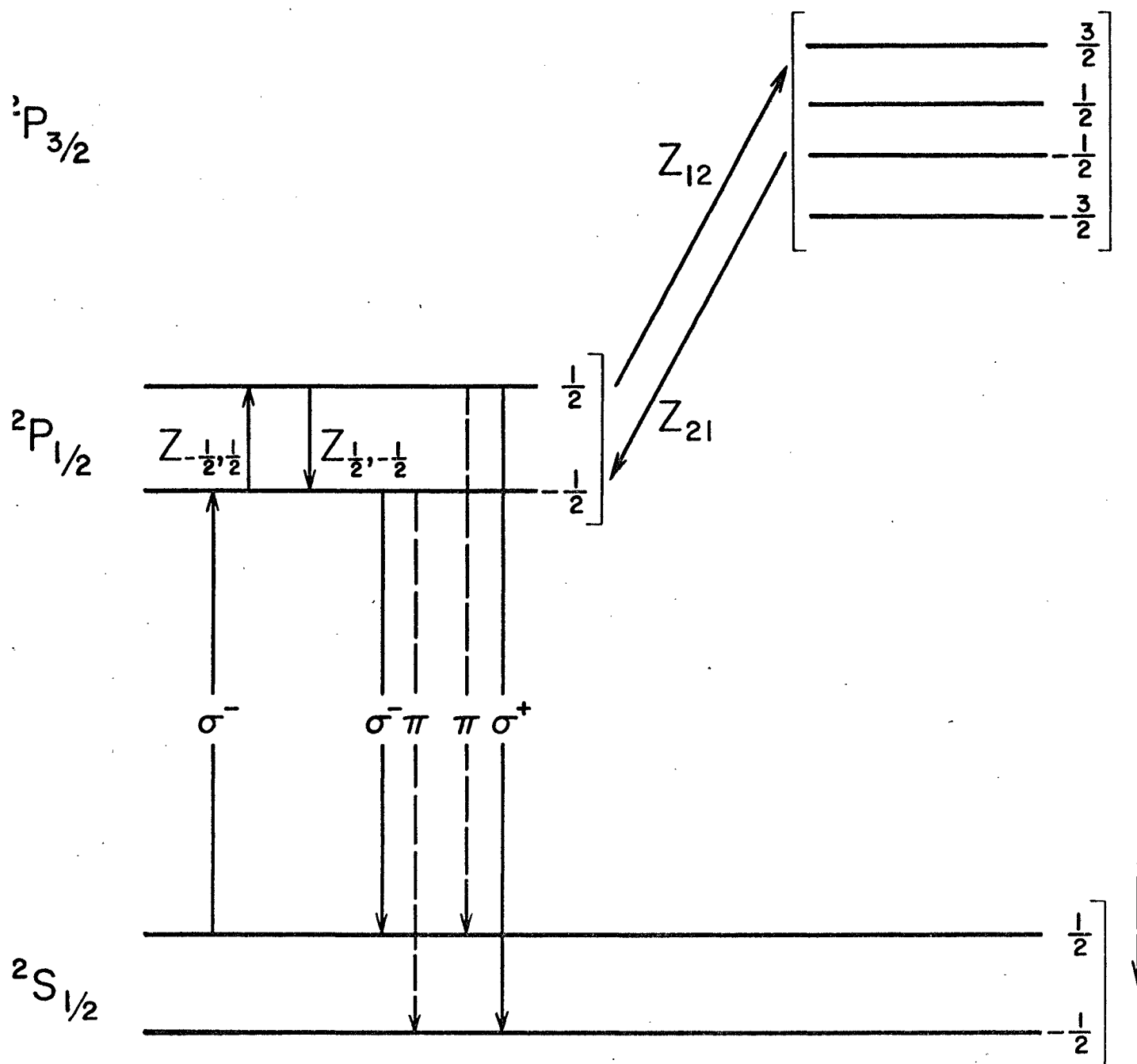


Fig. 3. Transitions between the Zeeman levels of the ground and resonance states. Broken lines indicate emissions not observed in the experiment.

UNIVERSITY OF WINDSOR LIBRARY

$$(4) \quad \frac{dN_2}{dt} = -\frac{1}{\tau} N_2 + Z_{12} (n_{-\frac{1}{2}} + n_{\frac{1}{2}}) - Z_{21} N_2 = 0,$$

where $\tau = 2.7 \times 10^{-8}$ sec is the average lifetime of the $^2P_{1/2}$ and $^2P_{3/2}$ states¹², N_1 and N_2 are the densities of the atoms in these states, Z_{12} and Z_{21} are the previously determined collision numbers (number of collisions per excited atom per second) corresponding to the transitions $^2P_{1/2} \rightarrow ^2P_{3/2}$ and $^2P_{1/2} \leftarrow ^2P_{3/2}$ ¹, respectively, $n_{\frac{1}{2}}$ and $n_{-\frac{1}{2}}$ are the densities of atoms in the $m_J = 1/2$ and $m_J = -1/2$ substates, respectively; $Z_{-\frac{1}{2}, \frac{1}{2}}$ and $Z_{\frac{1}{2}, -\frac{1}{2}}$ are the collision numbers corresponding to the m_J transitions $-1/2 \rightarrow 1/2$ and $1/2 \rightarrow -1/2$ within the $^2P_{1/2}$ state and $S_{-\frac{1}{2}}$ and $S_{\frac{1}{2}}$ are the densities of atoms excited per second to the $m_J = -1/2$ and $+1/2$ states, respectively. It is assumed that the effects of radiation trapping are negligible.

The addition of Equations (2) and (3) yields:

$$(5) \quad -\frac{1}{\tau} N_1 + Z_{21} N_2 - Z_{12} N_1 + S_1 = 0,$$

where $n_{-\frac{1}{2}} + n_{\frac{1}{2}} = N_1$ and $S_{-\frac{1}{2}} + S_{\frac{1}{2}} = S_1$. Equations (4) and (5) represent sensitized fluorescence arising from the collisional excitation transfer between the two resonance states⁶.

The $m_J = -1/2$ sublevel is selectively populated by exciting the atoms with radiation consisting principally of the σ^- component. From Equations (2) and (3), it is possible to calculate the ratio of the atomic densities $n_{\frac{1}{2}}$ and $n_{-\frac{1}{2}}$,

$$(6) \quad \frac{n_{\frac{1}{2}}}{n_{-\frac{1}{2}}} = \frac{(Z_{-\frac{1}{2}, \frac{1}{2}} + Z_{12} - \frac{1}{2} \eta_2 Z_{21} + \frac{1}{\tau})(S_{\frac{1}{2}}/S_{-\frac{1}{2}}) + Z_{-\frac{1}{2}, \frac{1}{2}} + \frac{1}{2} Z_{21} \eta_2}{(S_{\frac{1}{2}}/S_{-\frac{1}{2}})(Z_{\frac{1}{2}, -\frac{1}{2}} + \frac{1}{2} Z_{21} \eta_2) + \frac{1}{\tau} + Z_{\frac{1}{2}, -\frac{1}{2}} + Z_{12} - \frac{1}{2} Z_{21} \eta_2},$$

where $\eta_2 = N_2/N_1$.

The degree of circular polarization is defined in terms of the intensities, I_{σ^+} and I_{σ^-} , of the σ^+ and σ^- components present in the fluorescence.

$$(7) \quad P = \frac{I_{\sigma^-} - I_{\sigma^+}}{I_{\sigma^-} + I_{\sigma^+}} .$$

In the absence of depolarizing collisions,

$$(8) \quad P = P_0 = \frac{S_{-\frac{1}{2}} - S_{\frac{1}{2}}}{S_{-\frac{1}{2}} + S_{\frac{1}{2}}} .$$

The transition probabilities for the σ^+ and σ^- transitions are equal:

$$(9) \quad I_{\sigma^-} = A n_{-\frac{1}{2}} , \quad I_{\sigma^+} = A n_{\frac{1}{2}} ,$$

where A is the Einstein coefficient. Thus Equation (7) becomes:

$$(10) \quad P = \frac{1 - n_{\frac{1}{2}}/n_{-\frac{1}{2}}}{1 + n_{\frac{1}{2}}/n_{-\frac{1}{2}}} .$$

Substitution of Equation (6) into Equation (10) yields

$$(11) \quad P = P_0 \frac{1 + \tau Z_{12} - \tau Z_{21} \eta_2}{1 + \tau Z + \tau Z_{12}} ,$$

where $Z = Z_{-\frac{1}{2}, \frac{1}{2}} + Z_{\frac{1}{2}, -\frac{1}{2}}$. Equation (11) gives P, the degree of polarization of the fluorescence in a mixture of potassium vapour with an inert gas which, at low inert gas pressures, reduces to

$$(12) \quad P = P_0 \frac{1}{1 + \tau Z} ,$$

which is the Stern-Volmer Equation¹³. Using Equation (11), the

disorientation (m_J mixing) collision numbers can be determined from the degree of polarization, P , which is experimentally determined as a function of inert gas pressure. By analogy with classical gas kinetic theory, the total cross section, Q , for radiationless transfer between the two sublevels is given by

$$(13) \quad Q = \frac{Z}{N v_r} .$$

v_r is the average relative velocity of the colliding partners:

$$v_r = \sqrt{\frac{8kT}{\pi\mu}} ,$$

where μ is the reduced mass of the system.

From the principle of detailed balancing, $Z_{-\frac{1}{2}, \frac{1}{2}} = Z_{\frac{1}{2}, -\frac{1}{2}}$ because of the small energy defect ($\Delta E \ll kT$) and the equality of the statistical weights of the m_J sublevels.

IV. DESCRIPTION OF THE APPARATUS

The apparatus is shown schematically in Fig. 4. The potassium spectral lamp which was placed in a magnetic field, M_1 of 5 kG, emitted σ light parallel to the field. An interference filter selected the 7699 Å potassium resonance line and a $\lambda/4$ plate and polarizer separated the σ^+ or σ^- components. This light was made incident on a vapour-gas mixture contained in a fluorescence cell which was situated in a second, parallel, magnetic field, M_2 , variable from zero to 10 kG. Fluorescent light, observed along a direction parallel to the field M_2 , was passed through another interference filter, $\lambda/4$ plate and polarizer and was focused onto the photocathode of a cooled photomultiplier. The output of the latter was amplified and applied to the Y axis of the X-Y recorder, to whose X axis was applied the output of a gaussmeter which monitored the strength of the field M_2 .

(i) The Spectral Lamp

The light source has been described elsewhere¹⁴. It emitted resonance radiation from a horizontal pyrex tube three cm in length and 2.5 cm in diameter, which had plane end-windows and a side-arm 2.5 cm in length. The alkali vapour pressure was determined by the temperature of 0.5 g of distilled potassium contained in the side-arm appendage and the discharge was carried by 0.6 Torr of argon. The tube was placed completely in the tank coil of an rf

push-pull oscillator operated at 40 mc/sec. By maintaining a skin discharge at the proper temperatures, resonance lines of singular sharpness and intensity and with no self-reversal were produced.

(ii) The Electromagnets

Two 12 in. electromagnets, Magnion Model L-128A, mounted on wheeled carriages and arranged as shown in Fig. 5, were used in the experiment. The weight of each magnet exceeded 2.5 tons and required a minimum floor loading capacity of 1120 lbs. per sq. ft. Each yoke was inclined at 45° to the horizontal to permit easy access to the central field region. The coils had low impedance (one Ω) and were mounted in the yoke by means of three pins which were used in the alignment of the pole caps as well¹⁶. The pole caps fitted to magnet M_2 had central apertures two cm in diameter, which permitted fluorescence to be observed in directions parallel to the magnetic field. All pole caps were covered with thin teflon sheets as a precaution against damage.

The four in. gap which was used in both magnets, corresponded to a maximum field of 10 kG at 6.5 kW. The degree of homogeneity of the magnetic fields was quite acceptable. For magnet M_1 , the radial homogeneity approached one part in 10^4 over one in. Axial homogeneity was about one part in 3000 over one in. at 2600 gauss. As would be expected, the field of the magnet M_2 was distorted because of the apertures in the pole pieces. Radial homogeneity was equal to one part in 10^3 for the central field region over a distance of one in. The field homogeneity was investigated with an NMR probe in

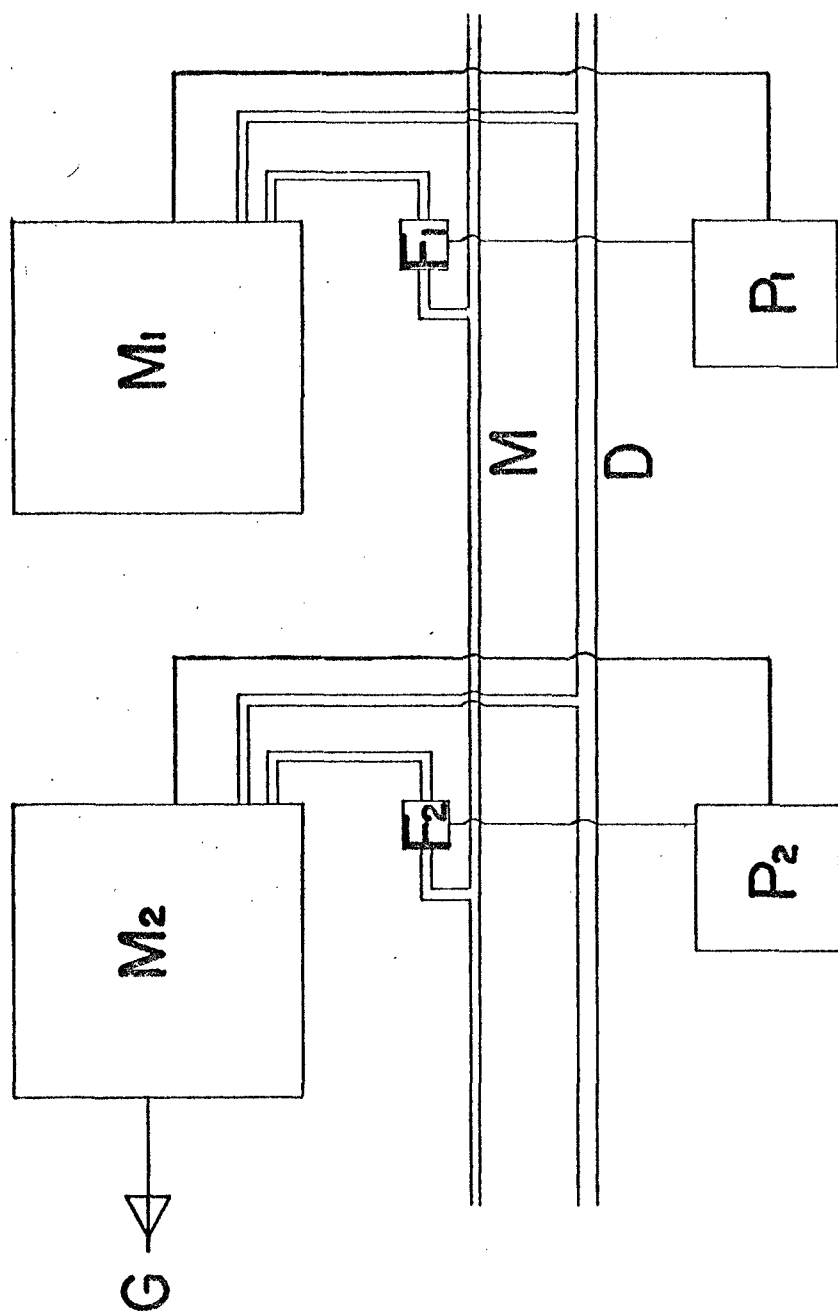


Fig. 5. Arrangement of the electromagnets. M_1, M_2 - magnets; P_1, P_2 - power supplies; F_1, F_2 - flow meters; M - water main; D - drain; G - gaussmeter.

conjunction with a calibrated gaussmeter.

The water cooling system, required for fields in excess of three kG, was capable of supplying two gal per min at pressures greater than 30 psi. The basic features are shown in Fig. 5: water taken from the main was passed through two "aqua pure" water filters in parallel which were installed in a 3/4 in. copper line. Two flow meters, McDonald and Miller type F34-3T3, were installed in 3/4 in. spur lines which immediately preceeded the magnets. The flow meters, with minimum actuation of two gal per min, were connected to the magnet power supplies which would be turned off if the flow rate should fall below the required amount.

The magnet power supplies, which have been previously described¹⁵, were the dc current regulated type with a maximum rating of 65 A at 130 V stable to one part in 10^4 . The helipots of both power supplies were fitted with slow, two-speed synchronous motor drives which permitted smooth scanning of the magnetic fields. When necessary, the motor drive could be disengaged by a spring loaded clutch to permit manual adjustment of the helipot setting. The magnetic fields were measured by an R.F.L. model 1890 gaussmeter which employed a hermetically sealed indium arsenide Hall probe. The gaussmeter was calibrated for zero and for the one kG range by using the internal reference magnet, and the probe was taped to the pole face of magnet M_2 , where its position was adjusted for maximum signal strength. Magnetic fields from 0.1 G to 20 kG could be measured with an accuracy of three per cent using 11 ranges. The

ambient temperature variation of the instrument was less than 0.1 per cent/ $^{\circ}\text{C}$ in the range of from -85°C to $+85^{\circ}\text{C}$. Because of this operating range, the probe could not be placed very close to the centre of the field which was to be occupied by the fluorescence cell enclosed in an oven. The gaussmeter was used to construct a calibration curve of magnetic field as a function of power supply helipot setting (range: 0 - 999).

(iii) The Fluorescence Cell

The fluorescence cell which resembled that used previously¹⁶, is represented diagrammatically in Fig. 6. The arrangement of three mutually perpendicular windows forming a rectangular corner permitted observation of fluorescent light emitted in directions either parallel or perpendicular to the magnetic field. Portions of the cell, especially near the actual corner, were coated with Aquadag. This reduced the effect of scattered light, limited observation to the region immediately adjacent to the corner and resulted in minimum reabsorption of both exciting and fluorescent light. The cell had a short side-arm which contained about 1.5 g of liquid potassium metal, and was connected to the vacuum and gas-filling system by a capillary one mm in diameter, attached directly above the side-arm. This arrangement ensured a good vacuum with little migration of alkali atoms which, though slight, often resulted in capillary occlusions which prevented accurate regulation of inert gas pressures in the cell. It was found that this situation could be corrected by enlarging the diameter of the capillary to two mm and by displacing its position a few mm with respect to that

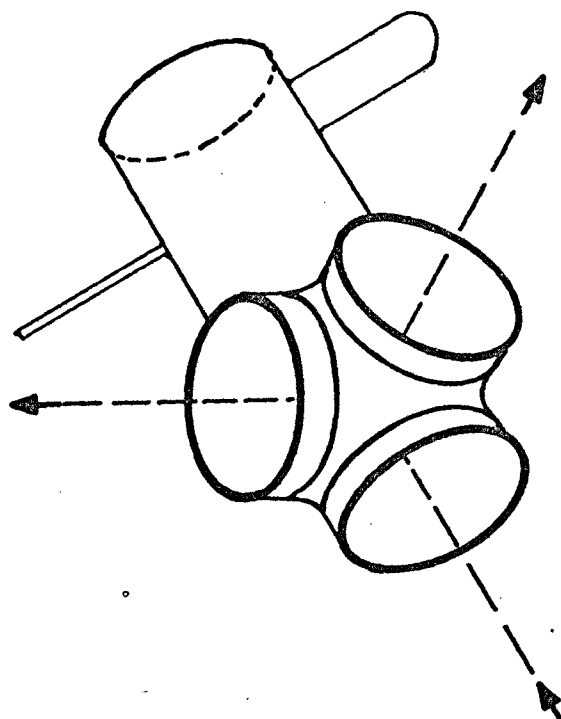


Fig. 6. Sketch of the fluorescence cell showing the location of the three mutually perpendicular windows, the side-arm and capillary connection. The arrows indicate the directions of excitation and of observation.

of the side-arm.

The fluorescence cell was enclosed in an oven, as shown in Fig. 7, and was mounted between the pole pieces of magnet M_2 . The oven consisted of two parts. The main part was a rectangular pannelite box with provisions made for access to the various cell windows and side-arm assembly. It was lined with asbestos paper and accommodated four heating elements placed along its sides, which were covered with one mm thick copper plate. The heating elements consisted of asbestos paper wound with No. 28 thermal heating wire and had a total parallel resistance of 4.8Ω . A side oven, consisting of a machined brass cylinder attached to the bottom of the main oven, was closely fitted to the side-arm with good thermal contact provided by an interposed layer of thin copper foil. Temperature stability, to within $\pm .25^\circ\text{C}$ was provided by a Jena Ultrathermostat which circulated hot water through a coil of $1/4$ in copper tubing snugly fitted to the side oven and thermally insulated by a layer of asbestos tape. Temperatures were measured by thermocouples which were affixed near the entrance and observation windows and near the side-arm of the cell and were connected to a Leeds and Northrup Model 8686 potentiometer. A thermistor attached to the base of the cell was connected to the temperature controller¹⁶ which was able to provide temperature stability of $\pm .5$ per cent in the range of from 50°C to 140°C .

(iv) The Optical System

The principal features of the optical system have been

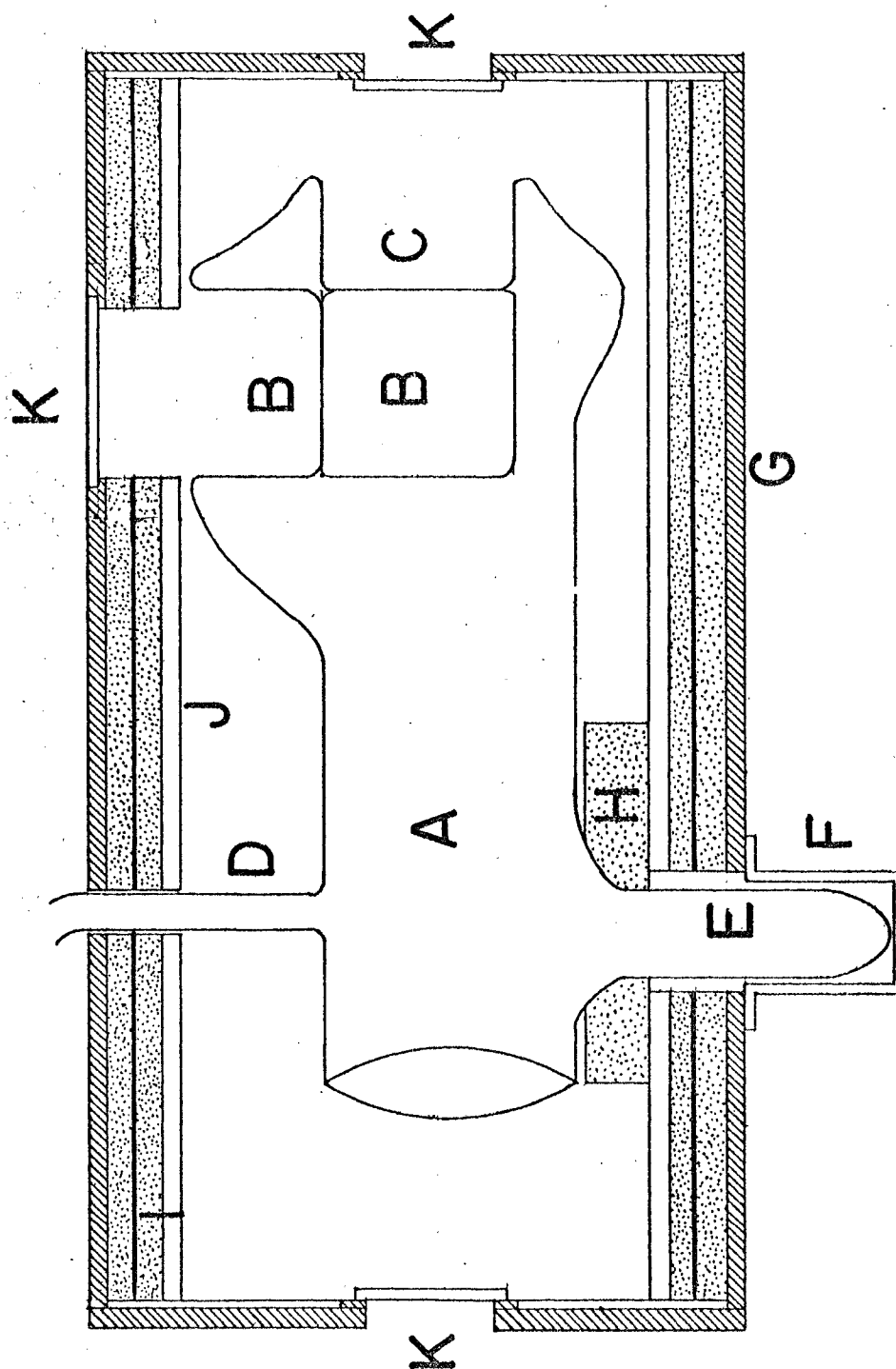


Fig. 7. The fluorescence cell in main oven. A - cell; B - observation windows; C - entrance window; D - capillary connection to the vacuum system; E - side-arm; F - side oven; G - panelyte; H - asbestos; I - heater wire; J - copper sheet; K - end windows.

outlined in Fig. 4. A totally reflecting right-angled prism was placed in the field M_1 to permit the emission of σ light in a direction parallel to that of the magnetic field. The interference filter, $\lambda/4$ plate and polarizer were placed in the exciting beam which was collimated by a double convex lens of 25 cm focal length; an identical lens condensed the parallel beam into the fluorescing region of the vapour. The interference filters (Spectrolab P type) transmitted 68 per cent of the 7699 Å radiation and less than 0.1 per cent of the 7665 Å radiation; the $\lambda/4$ plates used produced polarized light circular to within three per cent (based on ellipticity), while the polarizers were HNT polaroids with K_1 and K_2 transmissions of 55 per cent and less than one per cent, respectively, in the 7700 Å region. In the fluorescent light observed parallel to the field M_2 , the collimating lens had a focal length of 4.5 cm and a diameter of 1.8 cm. A brass adjustment tube, 50 cm in length, with inside and outside diameters of 17 and 19 mm, respectively, was reamed at one end to accept the lens which was held in place by a tension spring. The tube could slide freely in the pole piece aperture permitting ready adjustment of the lens position. All components were mounted on aluminum optical benches resting on demountable frames supported by the magnet carriage.

Fluorescent radiation was monitored by an FW118G, 16 dynode I.T.T. photomultiplier tube with an S-1(Ag-O-Cs) photocathode which has a peak sensitivity in the 8000 Å region. The photomultiplier, shielded against external magnetic and electric fields, was housed in a liquid air-cooled cryostat¹¹ and, as a result, had low background

noise. High voltage was generated by a Fluke 412B power supply operated at 1300 V through a resistive divider chain providing a 73 V drop per stage. The output was amplified by a Keithley model 417 high speed picoammeter fitted with variable damping and high suppression current adjustment. The latter feature permitted current suppression at the input of up to 1000 times full scale deflection, allowing large scale display of 0.1 per cent variation in the signal, thus eliminating most of the background noise which originated from dynodes other than the photocathode. The signal was then applied to the Y axis of a Hewlett-Packard model 2D X-Y plotter, the X axis of which was connected to the output of the gaussmeter.

(v) The Vacuum and Gas-Filling System

The vacuum system, a block diagram of which is shown in Fig. 8, was constructed of pyrex glass. The vacuum was attained by means of an Edwards water cooled oil diffusion pump model E02 operated with No. 704 silicone pumping fluid and backed by an Edwards single stage rotary pump model ES35. With a liquid air trap, the system produced vacua of the order of 10^{-7} Torr. Damage due to water and/or power failure was prevented by using a line relay switch in addition to an Edwards thermal switch on the diffusion pump which was also equipped with an Edwards electromagnetic backing valve.

The vacuum was measured with a C.V.C. model GIC-110 ionization gauge and an Autovac model 3294-B gauge was used for preliminary measurements of gas pressure. Final pressure readings were obtained with a C.V.C. model GM-100A trapped McLeod Gauge. When

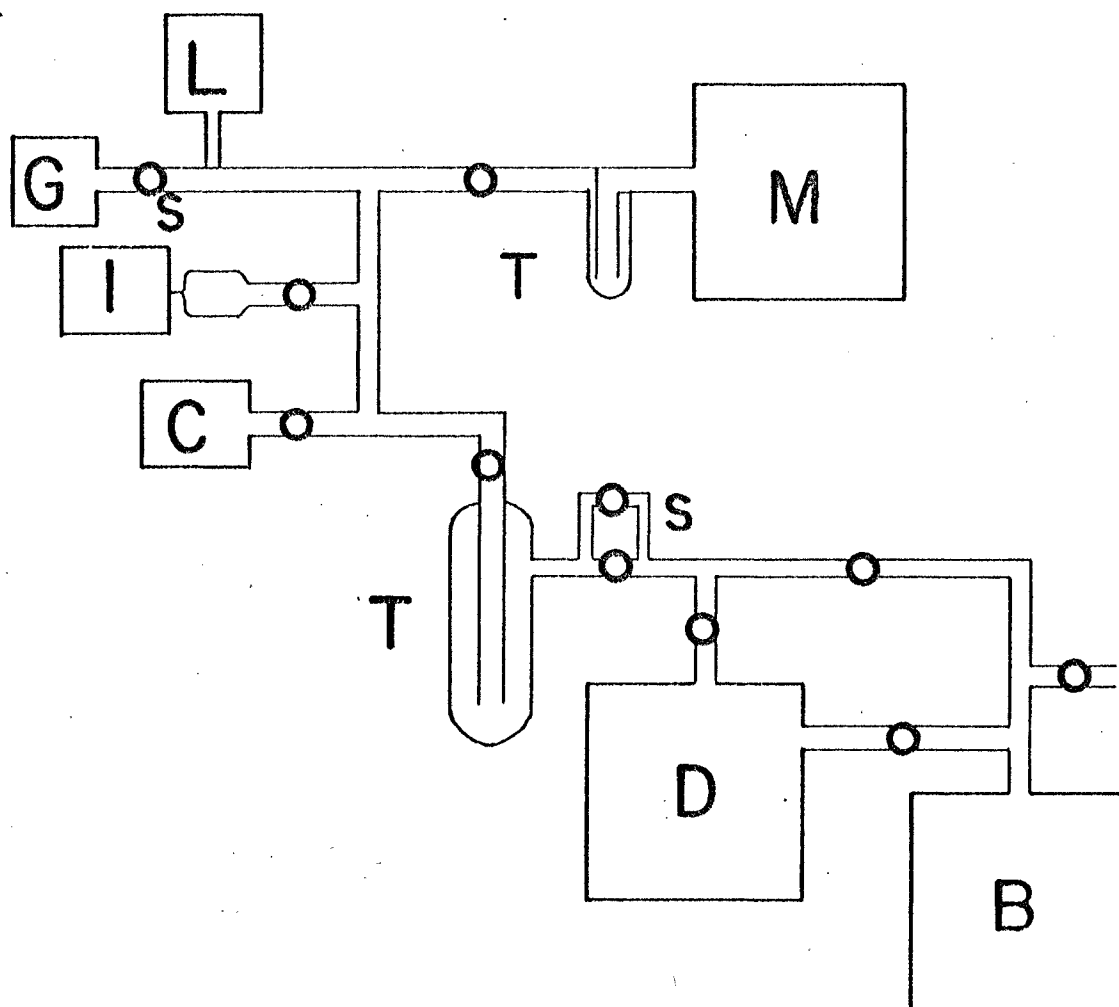


Fig. 8. The vacuum and gas-filling system. C - fluorescence cell; D - diffusion pump; B - backing pump; L - LKB gauge; I - ionization gauge; M - McLeod gauge; S - double flow stop cocks; T - trap.

not in actual use, the latter gauge was isolated from the system, to prevent contamination with mercury vapour.

The gas-filling assembly consisted of a dual stopcock, which permitted either slow or fast gas flow into the system, and a sealed pyrex flask containing the inert gas. The spectroscopically pure inert gases were supplied by the Linde Company, in one litre pyrex bulbs which could be sealed to the system and which, in the case of Kr and Xe, were fitted with cold traps.

The whole system was fastened to a rigid aluminum frame mounted on castors which straddled the pedestal mount of magnet M_2 and allowed easy and precise positioning of the fluorescence cell between the pole faces.

V. EXPERIMENTAL PROCEDURE

The configuration of the magnets was adjusted so that the surfaces of the right-hand (or left-hand) pole pieces were coplanar hence making the magnetic fields mutually parallel. This was done by using an aluminum optical bench as a straight edge for the pole piece surfaces.

The fluorescence cell was cleaned with dichromate cleaning solution and rinsed thoroughly with distilled water. It was then attached to the vacuum system and outgassed for several hours at a temperature of 150°C under a vacuum of 10^{-7} Torr. An ampoule containing 99.95 per cent pure potassium (supplied by the A. D. McKay Company) was broken under vacuum and about one g of the metal was distilled into the cell and side-arm. Distillation into the side-arm was completed by installing the cell in its oven in which a temperature of 150°C was maintained for several hours. During this time, the side-arm temperature was kept at 20°C by using the ultrathermostat to circulate cool water through the side oven coil. Thermistors and thermocouples were fastened in position using asbestos cement and the cell was properly enclosed in the oven. The operating temperatures of 95°C and 80°C for the main and side ovens, respectively, which were then established, produced a temperature gradient sufficient to prevent condensation of alkali vapour on the windows. The cell was positioned between the pole pieces of the magnet M_2 and its position

was adjusted, using a light beam which passed through both pole piece apertures, until the corner between the windows was clearly seen through one of the apertures.

The rf lamp was positioned between the pole pieces of magnet M_1 and the oscillator was set for maximum output (200 mA and 325-375 V) by adjusting the voltage and current of the input and by modifying the configuration of the tank coil with an insulated rod to change its capacitance¹¹. After the lamp had been glowing for a time sufficient to raise its temperature above 300°C (about 15-30 min), the temperature of its side-arm was adjusted (140-70°C depending on the age and condition of the lamp)¹¹. The cell temperatures were set at 95 and 80°C for the main and side ovens, respectively. An unresolved beam of potassium resonance radiation was directed at the cell and the resulting fluorescence was detected on the photomultiplier whose signal was registered on the linear scale of the picoammeter. The output of the latter was applied to the axes of the X-Y plotters and the signal fluctuations were used to determine the degree of linearity of the plotter, which was found to be satisfactory. The X axes of the recorders were calibrated in terms of the magnetic field strength using the output of the gaussmeter, by adjustment of the range controls for a varying magnetic field.

With the lamp and photomultipliers operating, interference filters were placed in the collimated portions of the beam. They and the lenses were adjusted separately until a maximum signal was indicated by the X-Y recorder. The lamp position was readjusted to improve the

signal strength and then the position of the prism used in perpendicular observation of the fluorescence was also appropriately adjusted. A field of five kG was applied to the lamp and, for excitation and observation perpendicular to the fields M_1 and M_2 , the resulting intensity, as indicated by the recorder, decreased significantly. The magnetic field M_2 was then slowly scanned from 0 to 10 kG and a recorder trace similar to that shown in Fig. 1 was obtained. The position of the elements in the optical system were then slightly readjusted to increase the height of the main maximum and to decrease the background. Polarizers were placed in the collimated beams of both the exciting and fluorescent light and were separately adjusted to produce maxima at about five kG for transmissions of vertically polarized σ light. From Fig. 1, it would be expected that the result should consist of a single peak of half the intensity at five kG. Furthermore, with the transmission axis of the polarizer oriented parallel to the magnetic field M_2 , an identical curve would result for π observation of the fluorescence. Fig. 2 shows that this is indeed the case except for a small peak at two kG. The fact that the two curves were identical indicated, that the 7699 Å resonance line was unpolarized, as expected. The $\lambda/4$ plates were then inserted into the collimated beam after the first and second azimuthal directions had been determined by using a reference $\lambda/4$ plate.

For observation and excitation parallel to the magnetic fields and with the $\lambda/4$ plate and polarizer adjusted to pass σ^- light in both the directions of excitation and observation, the magnetic

field M_2 was scanned to produce the intensity profile shown in Fig. 2. The $\lambda/4$ plate in the exciting beam was adjusted for minimal transmission of the unwanted σ^+ component by reversing the field M_2 and obtaining the least signal which arose from σ^+ fluorescence. The $\lambda/4$ plate in the fluorescent beam was adjusted similarly except that the magnetic field M_1 was reversed to obtain the minimal signal.

The procedure followed in an actual experimental run consisted of the following steps.

The fluorescence cell was completely evacuated and the magnetic field M_1 was set at five kG. The lamp was started and adjusted. For σ^- excitation and observation, the fluorescent intensity corresponding to the main peak in Fig. 2 was closely scrutinized. Lamp stability was determined by the behaviour of the peak height with time (a few hours were sometimes required to establish the desired degree of stability). The shape of the peak was usually quite sharp and any indications of broadening or self-reversal necessitated a decrease in the pressure of alkali vapour in the lamp achieved by a temperature decrease. It was found that a sharp line could become very broad and quite self-reversed if the temperature increased by 2-3°C in the vicinity of 137°C. After lamp stability was established, the magnetic field M_2 was scanned from zero to 10 kG and back, reversed, and scanned again. The main peak heights in the resulting recorder trace similar to that shown in Fig. 2, were used in the determination of the degree of polarization in conjunction with Equation (7). Although lamp intensity might vary over a one hour period (stability within three per cent for periods exceeding

45 min was usual) recording time for one trace was less than three min so that the important relative intensities of the two peaks remained essentially constant.

Inert gas was next introduced into the vacuum system and fluorescence cell. Equilibrium was established after a few seconds and the scanning procedure described above, was repeated at a series of pressures ranging from less than 0.2 Torr to about five Torr, resulting in intensity profiles similar to those shown in Fig. 9. For the heavier inert gases, especially at higher pressures, the time required for the attainment of equilibrium between the gas-filling system and the fluorescence cell increased markedly (for Xe at 6 Torr, 40 min was required). All inert gas pressures were adjusted using the slow leak valve located near the gas input in conjunction with a slow leak valve connected to the liquid air trap and diffusion pump.

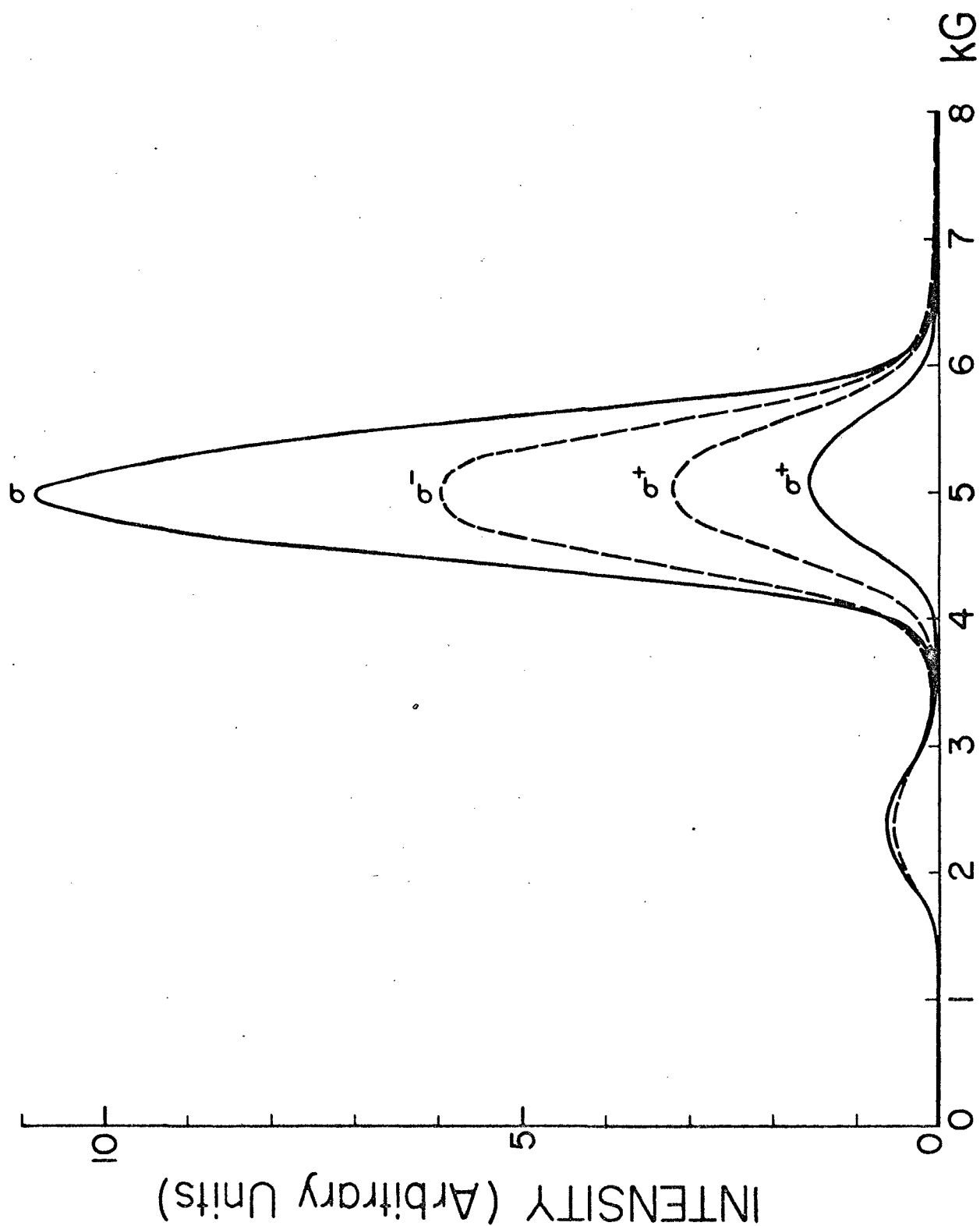


Fig. 9. Fluorescence from the $4^2P_{1/2}$ level in potassium vapor mixed with argon, excited with σ^- light. The σ^+ component arises from collisional m_j mixing. — 0.5 Torr; ---- 5.0 Torr.

VI. RESULTS AND DISCUSSION

The degrees of polarization of the resonance fluorescence observed in the various vapour gas mixtures are listed in Table I and are plotted as functions of inert gas pressures in Fig. 10. All the sets of values, each set obtained from at least two different runs to insure reproducibility, were substituted into Equation (11) to obtain the corresponding collision numbers $Z_{-\frac{1}{2},\frac{1}{2}}$ or $Z_{\frac{1}{2},-\frac{1}{2}}$. The values of η , Z_{12} and Z_{21} corresponding to the $4^2P_{1/2} \rightarrow 4^2P_{3/2}$ mixing process, were obtained from the previous work of Chapman¹⁶.

It may be seen in Fig. 10 that the degree of polarization in the absence of inert gas, P_0 , is not quite equal to unity. The magnitude of P_0 depends on the quality of the Zeeman components emitted by the lamp. For example, the curves for A and He are based on data obtained using a lamp filled with inert gas at a slightly lower pressure than was used in the other experiments. This would affect the operating characteristics of the lamp and would probably account for the observed differences in the values for P_0 . In addition, the operating conditions of each lamp change with time because of a decrease in the carrier gas pressure and the formation of a brown deposit on the windows of the lamp¹⁶. This latter effect would partially depolarize the emerging radiation and hence result in a slightly lower value of P_0 . Any depolarization due to circular polarizer inefficiency or collisions with cell walls appeared to have little effect on the atomic orientation.

TABLE I

Collision Cross Section for $m_J = -1/2$ — $m_J = 1/2$ Mixing
in the $4^2P_{1/2}$ State of Potassium

Collision Partners	Inert Gas Pressure (Torr)	Degree of Polarization	Collision Numbers $Z_{-1/2, -1/2}$ or $Z_{1/2, -1/2}$ (sec^{-1}) $\times 10^{-6}$	Collision Cross Sections $Q_{-1/2, -1/2}$ or $Q_{1/2, -1/2}$ (\AA^2)	Average Cross Section $\bar{Q}_{-1/2, -1/2}$ or $\bar{Q}_{1/2, -1/2}$ (\AA^2)
K - HE	0.00	0.882	-	-	
	0.06	0.845	0.82 *	35.54 *	
	0.16	0.770	2.82 *	45.82 *	
	0.30	0.692	5.04	47.94	
	0.53	0.615	9.13	44.76	
	0.79	0.535	14.44	47.45	46.0
	1.20	0.457	20.94	45.31	
	1.85	0.368	32.99	46.31	
	2.50	0.321	42.27	43.91	
	3.85	0.257	60.90 *	41.07 *	
	5.00	0.220	76.84 *	38.90 *	
K - NE	0.00	0.860	-	-	
	0.06	0.843	0.37 *	33.83 *	
	0.11	0.814	1.05 *	47.53 *	
	0.29	0.757	2.56	43.82	
	0.53	0.701	4.33	40.34	
	1.02	0.620	7.62	37.12	39.3
	1.45	0.548	11.49	39.34	
	2.25	0.479	16.62	36.68	
	3.45	0.386	26.76	38.51	
	4.55	0.345	33.51 *	36.55 *	
	5.55	0.319	38.54 *	35.41 *	
K - A	0.00	0.879	-	-	
	0.06	0.860	0.41	41.83 *	
	0.11	0.840	0.87	48.26 *	
	0.28	0.780	2.42	52.76	
	0.55	0.710	4.68	51.89	
	1.16	0.590	9.98	52.49	52.4
	1.80	0.500	16.72	56.63	
	2.52	0.456	20.82	50.38	
	3.45	0.396	28.27	49.92	
	4.32	0.362	34.04	48.04 *	
	5.36	0.326	41.79	47.53 *	

(Table continued on next page)

Table I - Collision Cross Section for $m_J = -1/2$ — $m_J = 1/2$ Mixing in the $4^2P_{1/2}$ State of Potassium (continued)

Collision Partners	Inert Gas Pressure (Torr)	Degree of Polarization	Collision Numbers $Z_{-\frac{1}{2},\frac{1}{2}}$ or $Z_{\frac{1}{2},-\frac{1}{2}}$ (sec^{-1}) $\times 10^{-6}$	Collision Cross Sections $Q_{-\frac{1}{2},\frac{1}{2}}$ or $Q_{\frac{1}{2},-\frac{1}{2}}$ (\AA^2)	Average Cross Section $Q_{-\frac{1}{2},\frac{1}{2}}$ or $Q_{\frac{1}{2},-\frac{1}{2}}$ (\AA^2)
K - KR	0.00	0.863	-	-	
	0.06	0.834	0.61	76.75 *	
	0.11	0.796	1.54	94.98 *	
	0.32	0.740	3.15	69.58 *	
	0.50	0.673	5.52	76.29	
	1.10	0.540	12.61	79.84	78.6
	1.50	0.485	17.09	79.38	
	1.72	0.449	20.76	84.08	
	2.20	0.416	25.02	79.22	
	3.10	0.348	36.35	81.67	
	4.33	0.301	47.87	77.01 *	
	5.25	0.264	58.85	78.08 *	
K - XE	0.00	0.862	-	-	
	0.05	0.826	0.82 *	128.21 *	
	0.10	0.797	1.55 *	111.13 *	
	0.31	0.716	4.01	096.21	
	0.48	0.646	6.80	105.21	
	0.94	0.517	14.61	115.33	107.9
	1.55	0.432	23.33	111.12	
	2.03	0.386	30.00	109.13	
	3.45	0.291	51.23	109.63	
	4.20	0.264	60.91 *	107.05 *	
	5.70	0.232	74.26 *	096.19 *	

* Results not included in the averaging process.

Main Oven Temperature: 95°C

Side Oven Temperature: 81 - 82°C

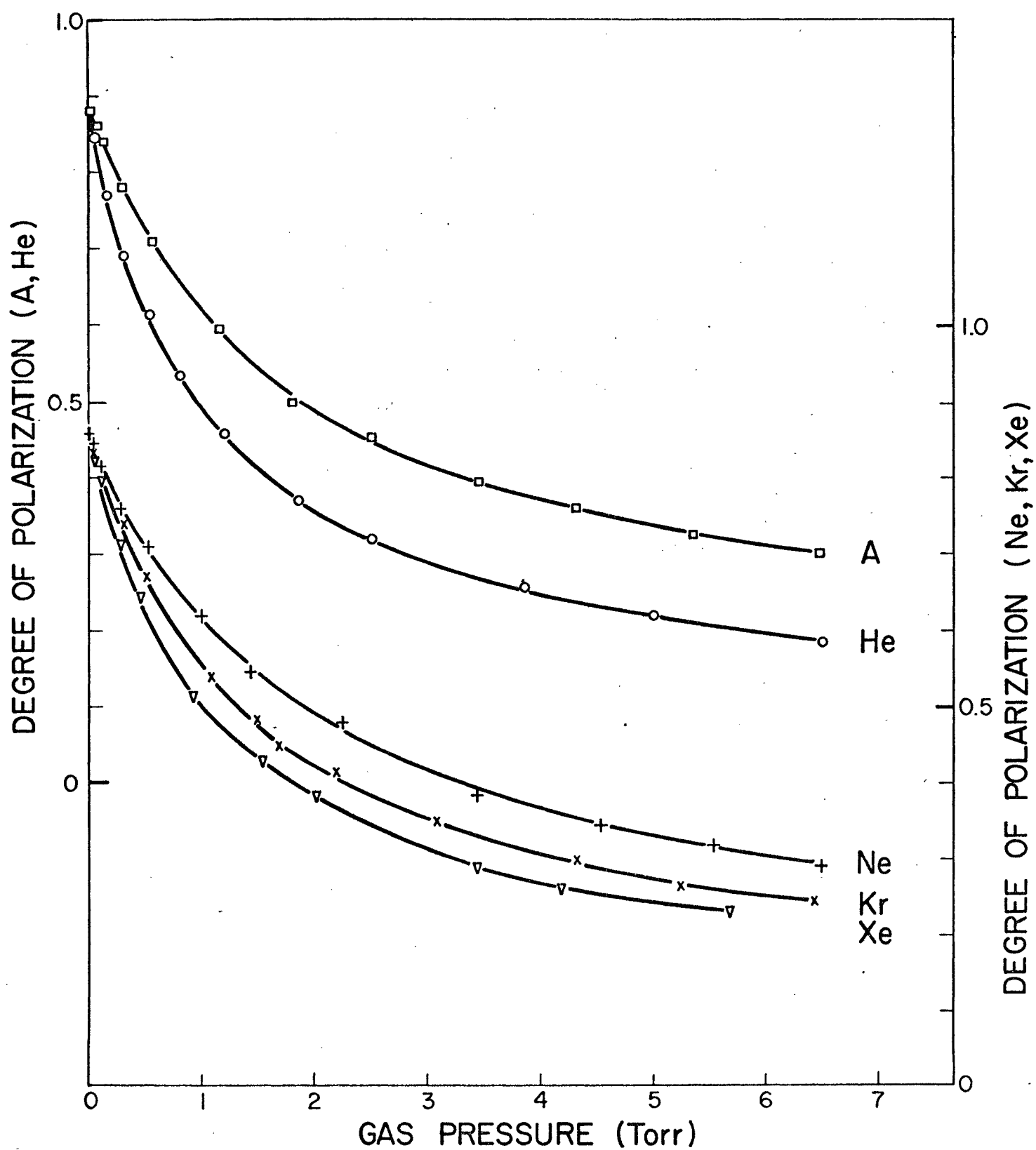


Fig. 10 The degrees of polarization of the 7699 Å resonance fluorescence, plotted as functions of inert gas pressures.

The variations of the collision numbers with inert gas pressure, along with an additional plot for neon obtained using Equation (12) in which the transitions $^2P_{1/2} \rightarrow ^2P_{3/2}$ have been neglected, are shown in Fig. 11. The cross sections $Q_{-\frac{1}{2}, \frac{1}{2}}$ or $Q_{\frac{1}{2}, -\frac{1}{2}}$ were determined in a series of point by point calculations using Equation (13) and all the experimental data. The final values for $Q_{-\frac{1}{2}, \frac{1}{2}}$ or $Q_{\frac{1}{2}, -\frac{1}{2}}$ were obtained by averaging the individual values for each gas. With the exception of a few experimental points which were judged unreliable, all the individual cross sections for a given gas agreed with each other to within five per cent.

The variations of collision numbers with inert gas pressures are linear up to pressures of six Torr. Above this pressure, however, the deviation from linearity becomes increasingly pronounced. The exact cause of this deviation is not known but is thought to arise from the fact that Equation (11) becomes increasingly approximate since terms pertaining to transitions between the $^2P_{1/2}$ and $^2P_{3/2}$ resonance states do not take into account m_J mixing in the $^2P_{3/2}$ state which will be reflected in any selection rules governing collisional transitions. The variation of collision numbers with low inert gas pressure also displays a non-linearity arising from relatively small differences between P_0 and P , to which the collision number is proportional. The plot of collision numbers against inert gas pressure according to the Stern-Volmer formula (the broken curve in Fig. 11) becomes non-linear in the region of one Torr. This is due principally to the fact that the Stern-Volmer formula does not allow for transitions between the

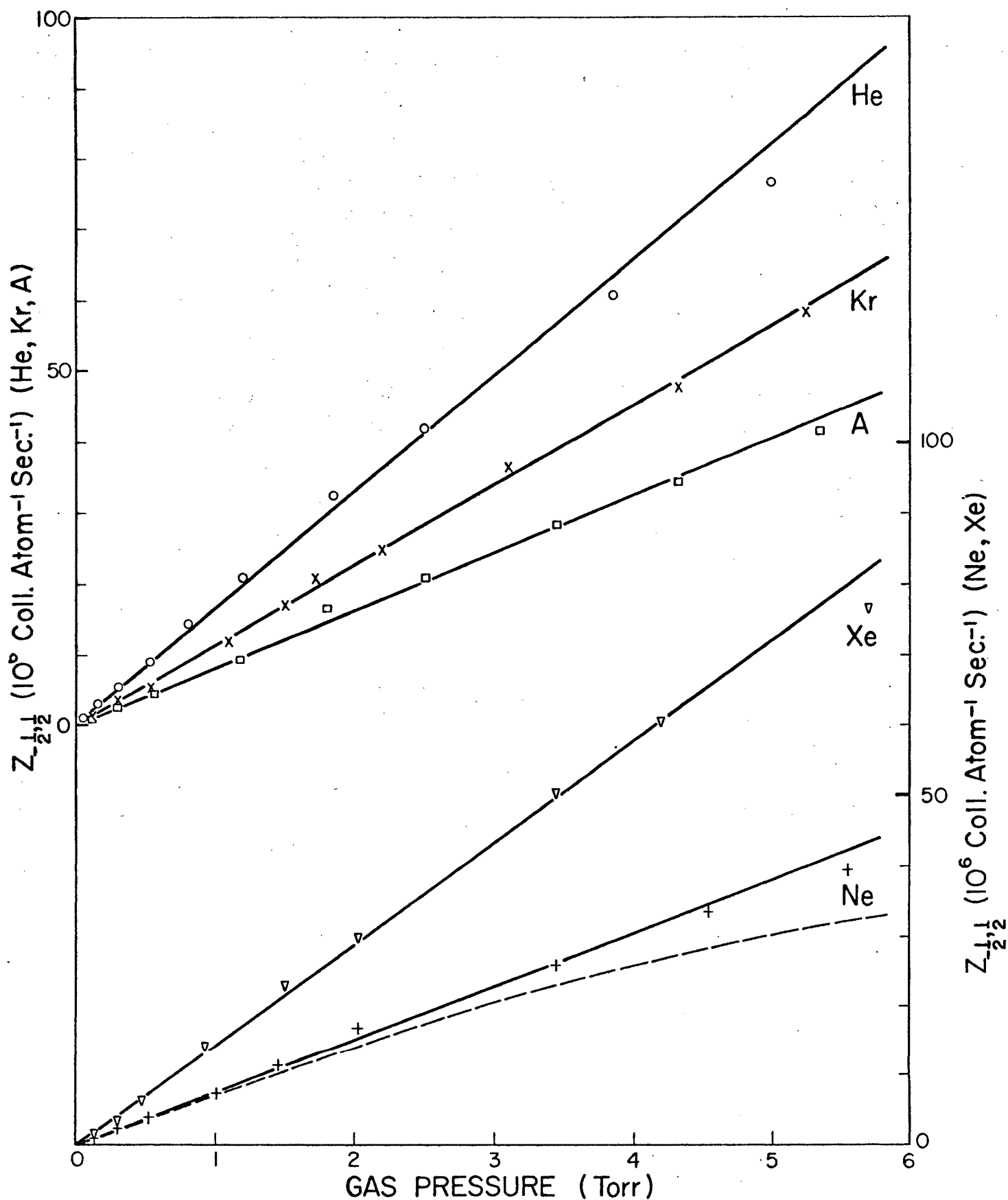


Fig. 11. Plots of collision numbers against the pressures of the inert gases. The broken curve results from a treatment which neglects $p_{i/2}$ mixing.

two fine structure resonance states.

It might be considered noteworthy that the cross sections reported here are of the same order of magnitude as recently determined alignment depolarization cross sections for the lowest 3P_1 level of cadmium perturbed by inert gases¹⁷.

Fig. 12 shows the variation of the total cross section with atomic number of the inert gases and also a similar plot for elastic electron scattering cross sections¹⁸. The magnitudes of the cross sections of these two cases are different but each plot exhibits the same general behaviour as observed in the cases of $^2P_{1/2} \rightarrow ^2P_{3/2}$ mixing collisions between potassium, rubidium or cesium and inert gas atoms⁶. Collisional interactions leading to $^2P_{1/2} \rightarrow ^2P_{3/2}$ excitation transfer have been interpreted as taking place between inert gas atoms and alkali atoms behaving as quasi free particles. Fig. 12 suggests that a similar mechanism might govern the collisional m_J mixing process.

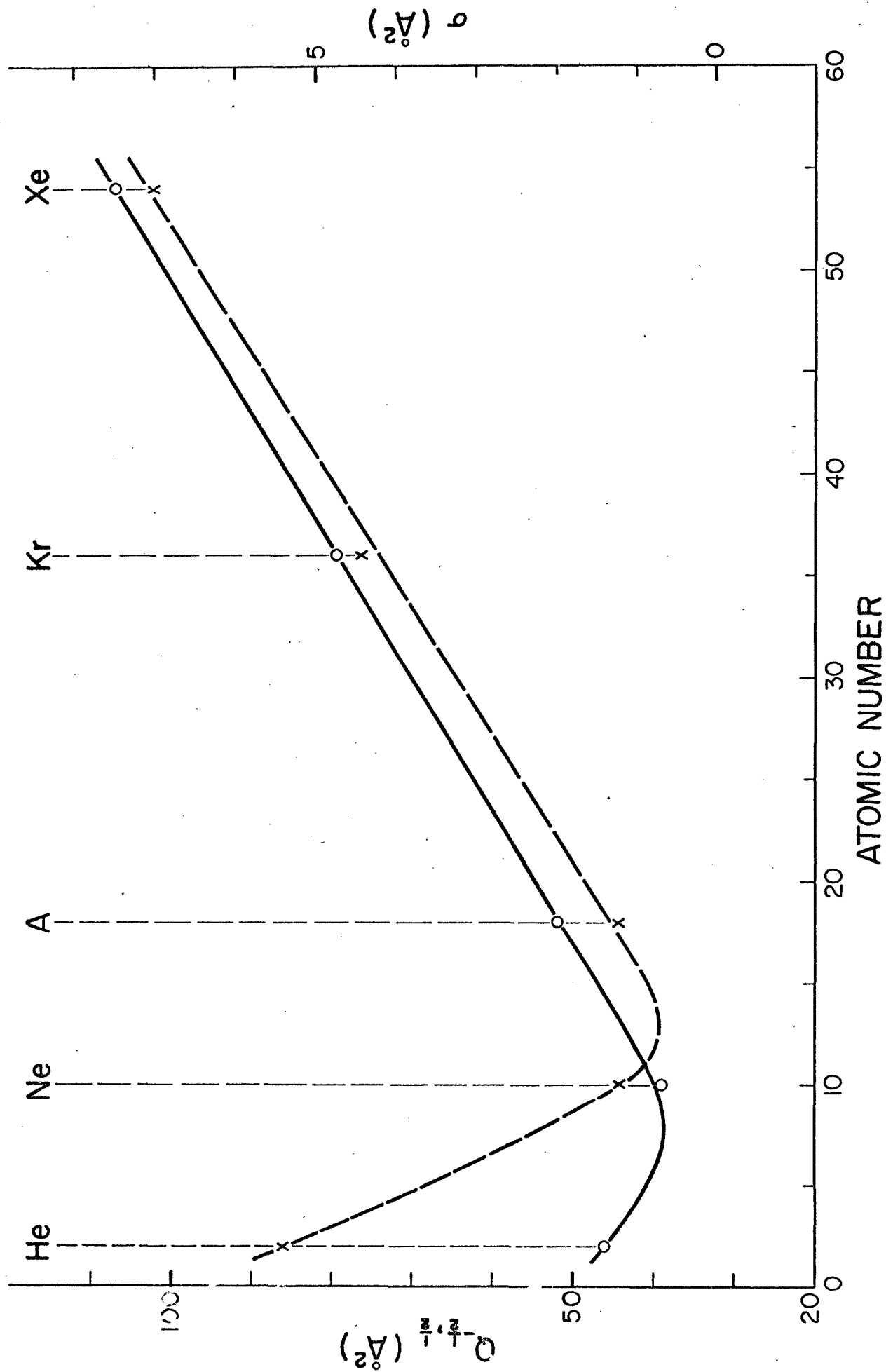


Fig. 12. A comparison of the disorientation cross sections $Q_{\frac{1}{2}, \frac{1}{2}}$ for potassium-inert gas collisions with the elastic electron scattering cross sections $\sigma(0, Q_{\frac{1}{2}, \frac{1}{2}}; x, \sigma)$. No physical dependence of the cross sections on the atomic number is implied.

BIBLIOGRAPHY

1. G. D. Chapman and L. Krause, Can. J. Phys. 44, 753 (1966).
2. A. G. A. Rae and L. Krause, Can. J. Phys. 43, 1574 (1965).
3. M. Czajkowski and L. Krause, Can. J. Phys. 43, 1259 (1965).
4. B. Pitre, A. G. A. Rae and L. Krause, Can. J. Phys. 44, 731 (1966).
5. M. Czajkowski, D. McGillis and L. Krause, Can. J. Phys. 44, 91 (1966).
6. L. Krause, Appl. Optics 5, 1375 (1966).
7. F. A. Franz and J. R. Franz, Phys. Rev. 148-1, 82 (1966).
8. W. Gough, Proc. Phys. Soc. 90, 287 (1967).
9. K. G. Kessler, Physica 33, 29 (1967).
10. Some preliminary results dealing with the disorientation of the $4^2P_{3/2}$ potassium atoms by collisions with He, appear in Proceedings of the XX Colloque Ampere (North Holland Publishing Company, 1967).
11. T. Shiner, M.Sc. Thesis, University of Windsor (1967).
12. G. Stephenson, Proc. Phys. Soc. A64, 458 (1951).
13. D. Stern and M. Volmer, Physik. Z. 20, 183 (1919).
14. W. Berdowski, T. Shiner and L. Krause, Appl. Optics (to be published).
15. John D. Colclough, M.Sc. Thesis, Assumption University of Windsor (1963).
16. G. D. Chapman, Ph.D. Thesis, University of Windsor (1966).
17. R. L. Barger, Phys. Rev. 154-1, 94 (1967).
18. H. S. W. Massey and E. H. S. Burhop, Electronic and Ionic Impact Phenomena (Oxford University Press, Oxford, 1952).

VITA AUCTORIS

I was born on February 18, 1944 in Chatham, Ontario. I attended primary and secondary schools in Windsor, Ontario and, after graduation in 1962, I attended the University of Windsor. In 1965, I graduated from an Honours Physics course and enrolled in the Faculty of Graduate Studies to work toward a Master of Science degree.